

Fig. 1. Arrangement for phase-shifting digital holography: BS1, BS2, beam splitters; M, mirror.

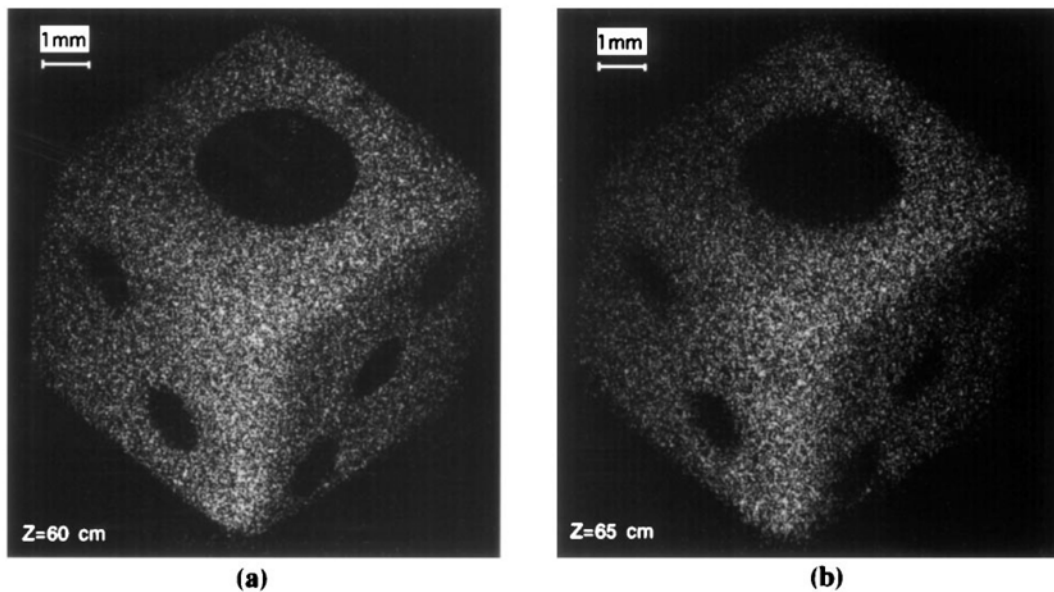


Fig. 5. Numerically reconstructed images of a diffusely reflecting object: (a) focused image, (b) defocused image.

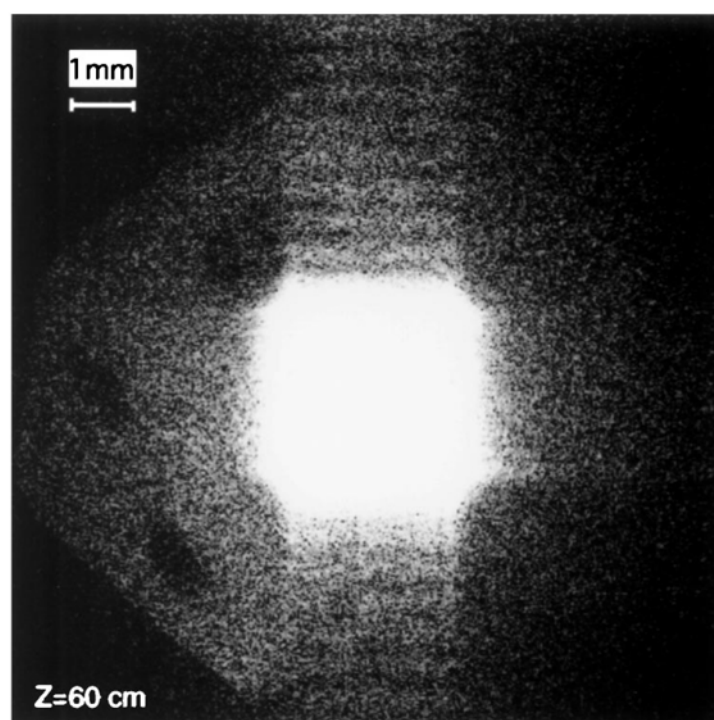


Fig. 6. Reconstructed image from a single interference pattern corresponding to a Gabor hologram.

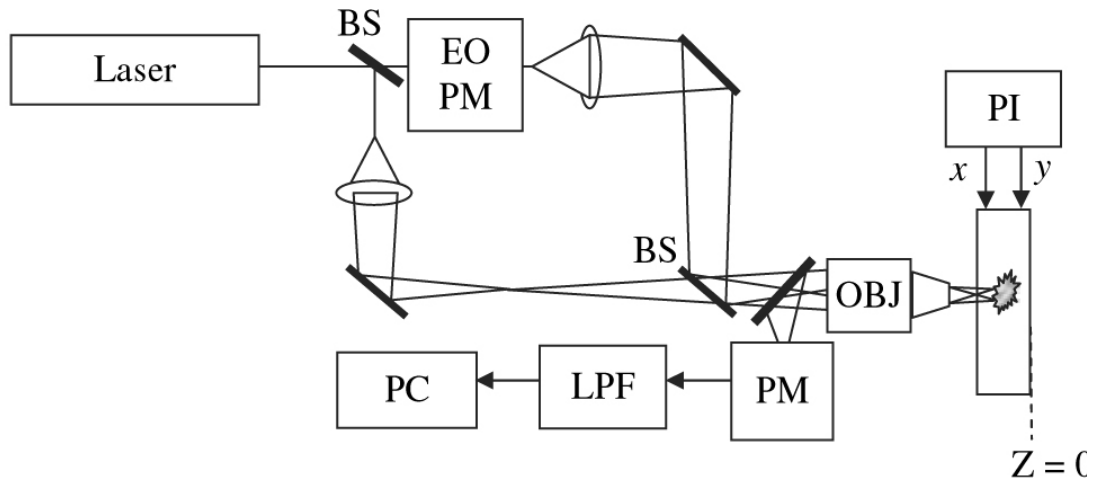


Fig. 3. Optical setup of the homodyne scanning holography system EOPM, electro-optic phase modulator introducing a phase difference between the two beams; BS, beam splitter; PI, piezo XY stage, OB, objective; PM, photomultiplier tube detector; LPF, lowpass filter; PC personal computer.

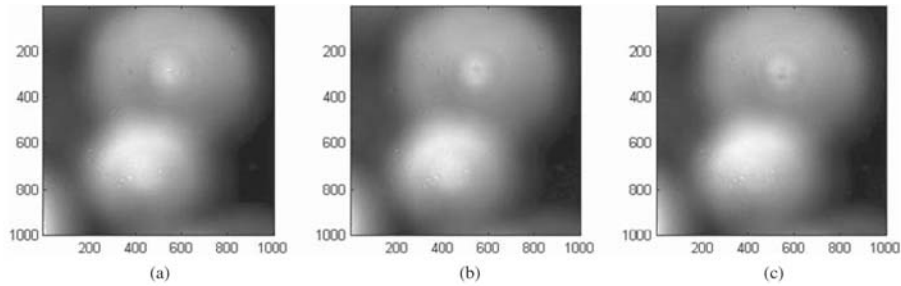


Fig. 4. Three recorded holograms with phase difference between the two interferometers arms of (a) 0, (b) $\pi/2$, and (c) π , all obtained from the homodyne scanning holography system.

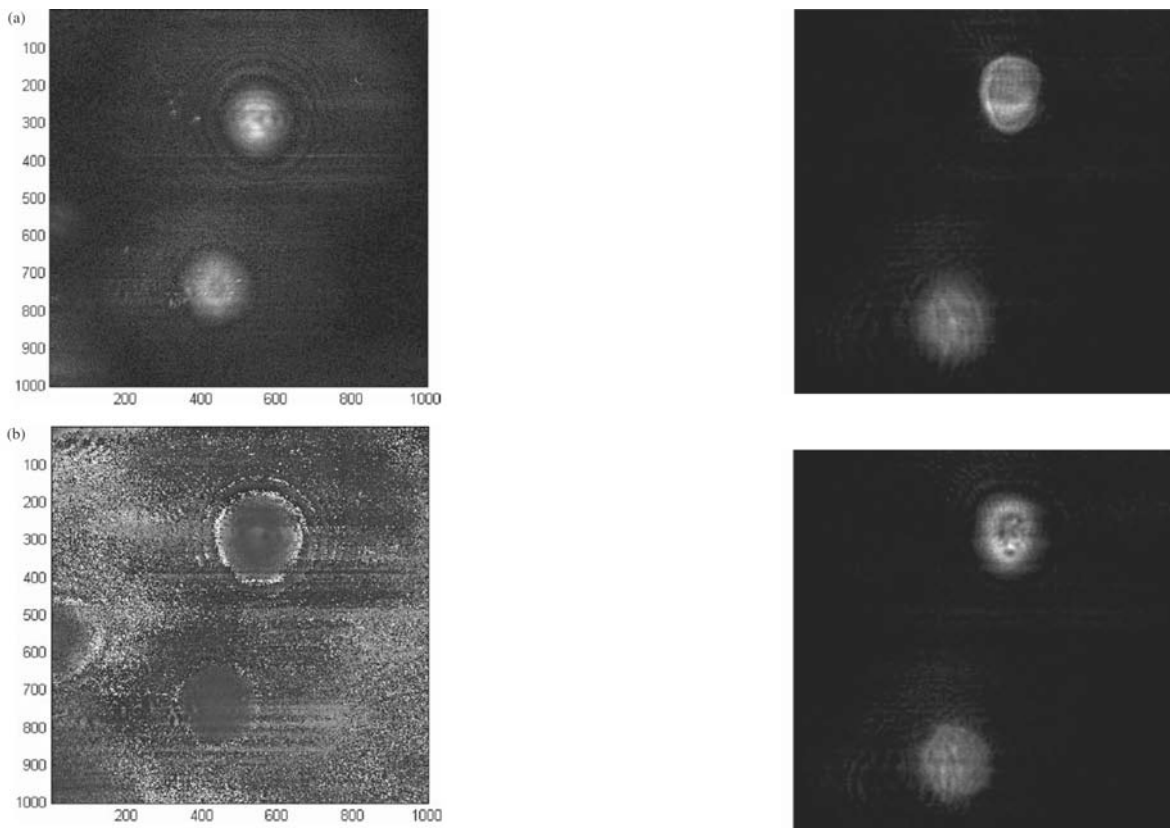


Fig. 5. (a) The magnitude and (b) the phase of the final homodyne scanning hologram.

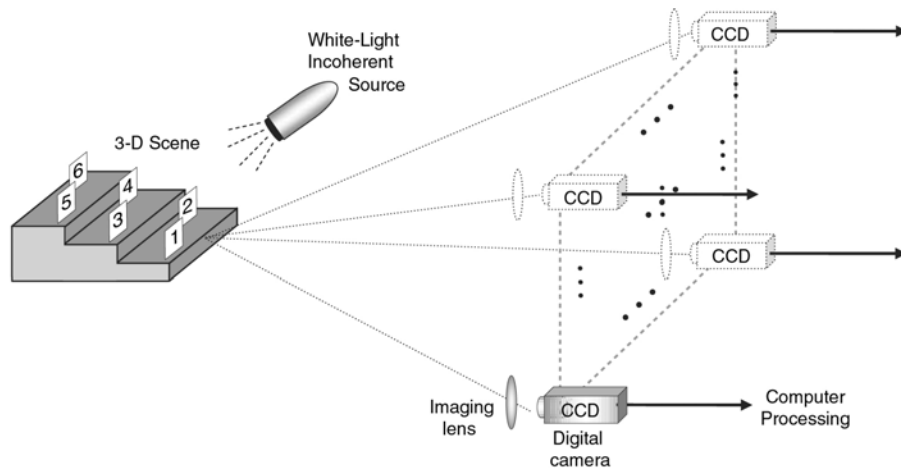


Fig. 7. Optical system for capturing multiple-viewpoint projections of the 3-D scene for obtaining a two-dimensional DIMFH of the scene. T camera and its imaging lens move together into a different capturing viewpoint for each projection.

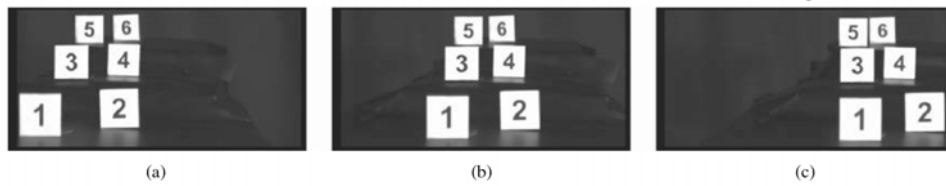


Fig. 9. (a-c) Three projections taken from the entire projection set obtained by the system shown in Figure 7, but with horizontal movement only the camera.

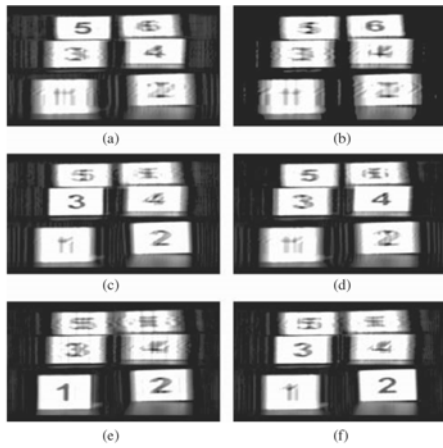


Fig. 11. (a-f) The six best in-focus reconstructed planes along the optical axis obtained by digital reconstruction from the hologram of Figure 10.

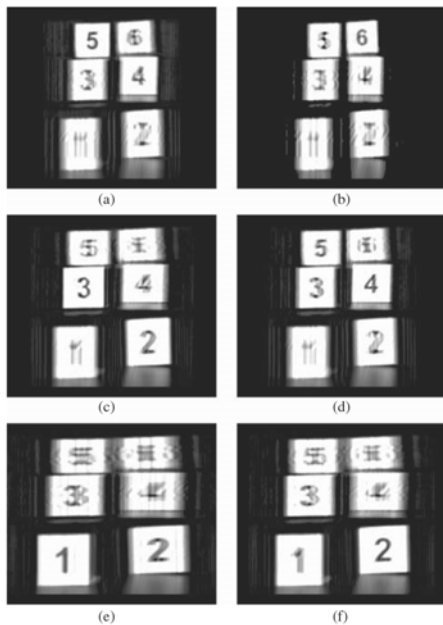


Fig. 12. (a-f) The six best in-focus reconstructed planes along the optical axis, obtained by digital reconstruction from the hologram of Figure 10, after the rescaling process of the horizontal axis.

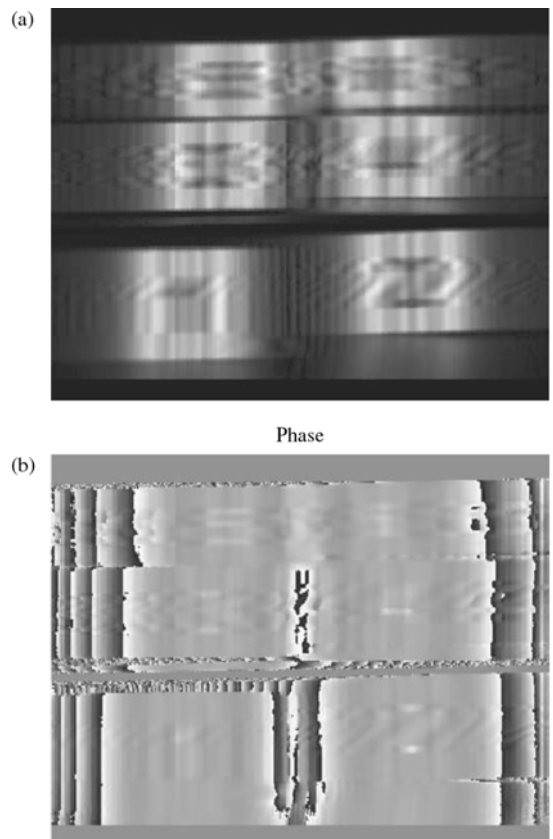


Fig. 10. (a) Magnitude and (b) phase of the one-dimensional DIMFH

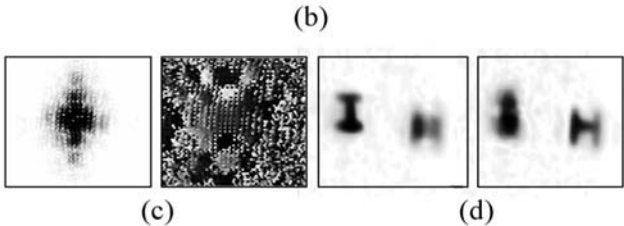
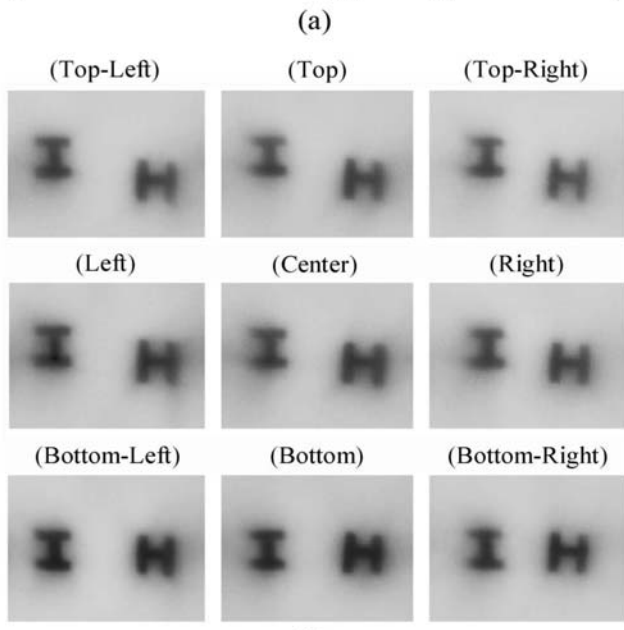
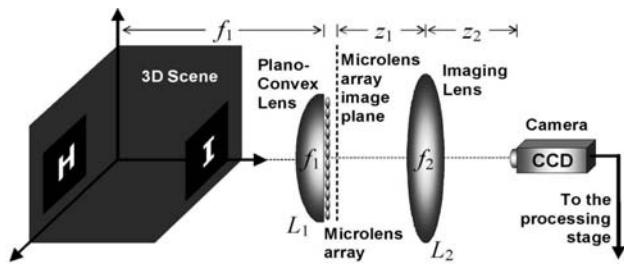


Fig. 1. Integral holography—MVP holography using a microlens array [29]. (a) Optical system for capturing the MVPs. (b) Several projections taken from different parts of the microlens array image plane captured by the camera. Larger part of this image plane is shown in View 1 and Media 1. (c) Magnitude (left) and phase (right) of the 2-D Fourier hologram obtained after performing the processing stage on the captured projections; (d) Best-in-focus reconstructed planes obtained by digital Fresnel propagation. Note that (b)–(d) are contrast-inverted. The continuous Fresnel propagation as 2-D slices and the entire reconstructed volume are shown in View 2, as well as in Media 2 and Media 3 (best-in-focus axial points are amplified).

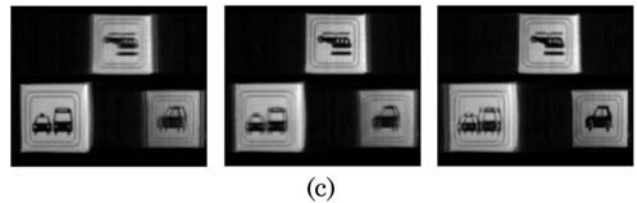
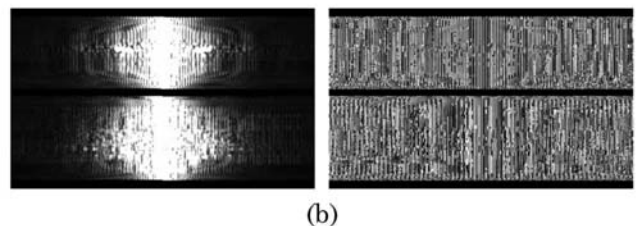
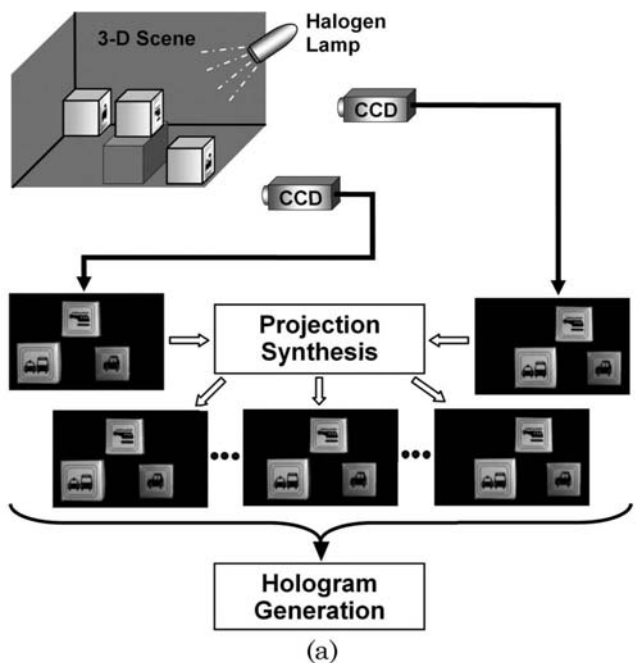


Fig. 2. Synthetic projection holography (SPH)—optically acquiring only a small number of projections and synthesizing the middle MVPs by the view synthesis algorithm [33]: (a) Schematics of the experimental setup. Only two projections are optically acquired. The entire MVP set (including the synthesized projections) is shown in View 3 and Media 4. (b) Magnitude (left) and phase (right) of the 1-D Fourier hologram obtained from the final set of MVPs. (c) Best-in-focus reconstructed planes. The continuous Fresnel propagation as 2-D slices and the entire reconstructed volume are shown in View 4, as well as in Media 5 and Media 6 (best in focus axial points are amplified).

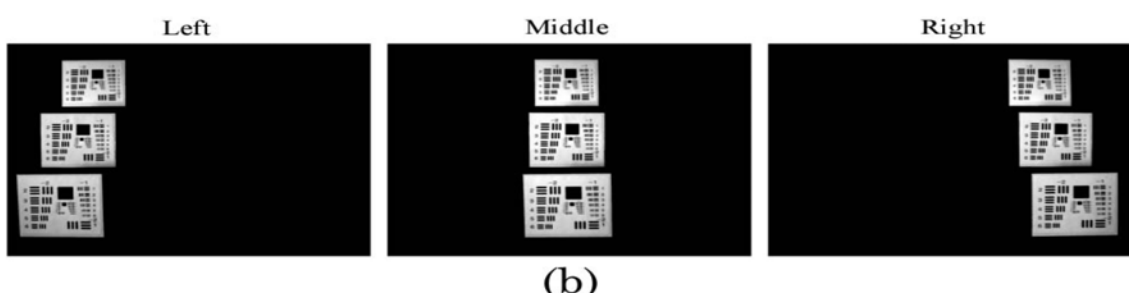
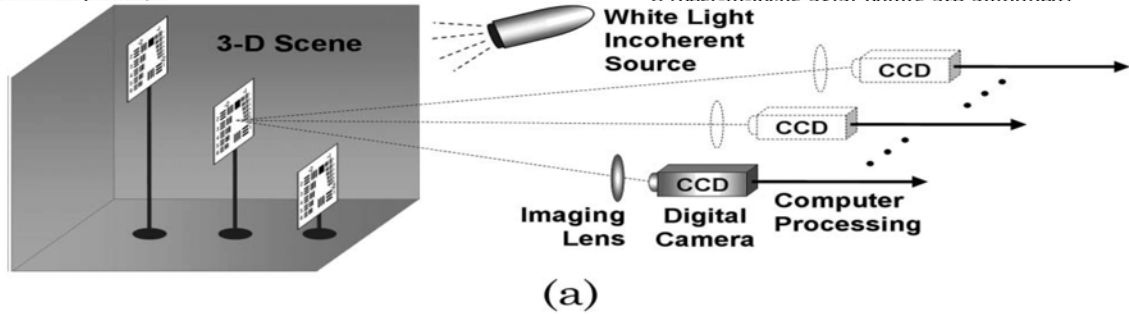


Fig. 4. 1-D MVP holography [38]: (a) Optical system for acquiring MVPs of a 3-D scene along the horizontal axis. (b) Several projections taken from the entire set of 1200 projections, which are shown in View 5 and Media 7.

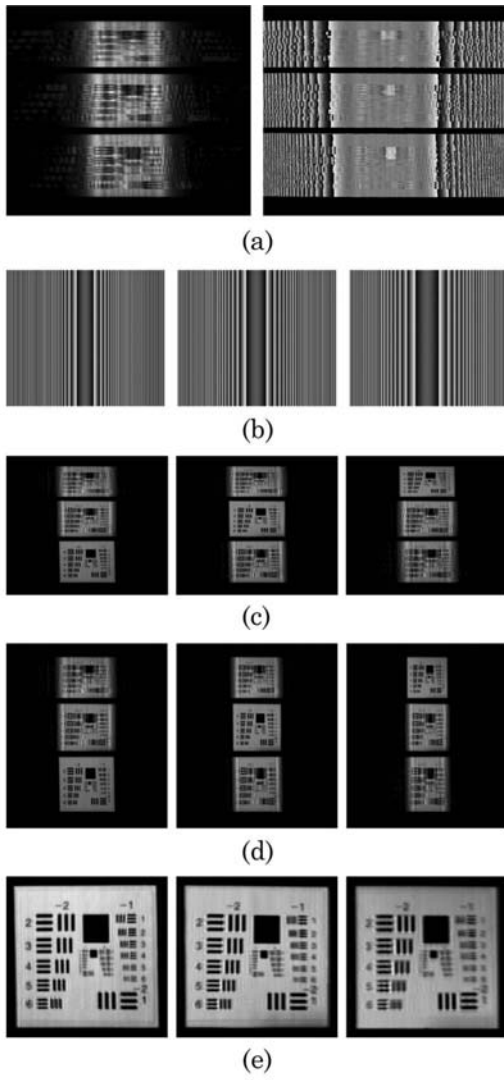
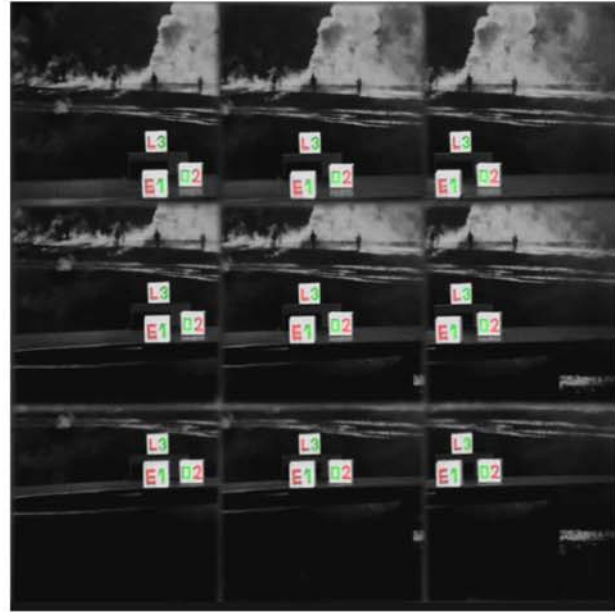
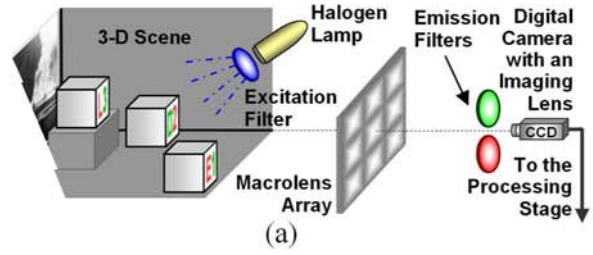
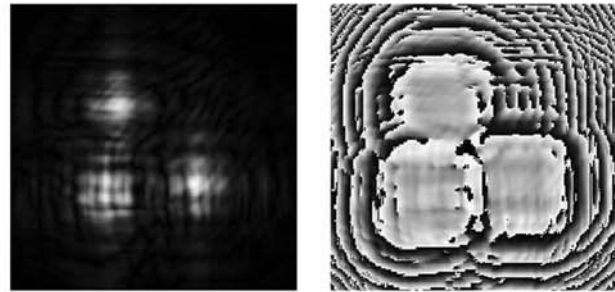


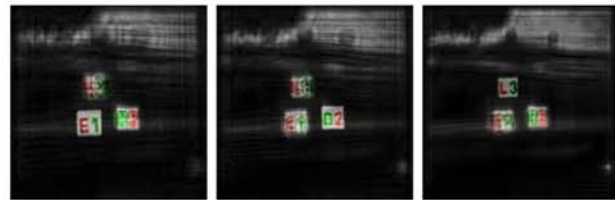
Fig. 5. One-dimensional DIMFH results obtained from the MVP set, partially shown in Fig. 4(b) [38]: (a) Magnitude (left) and phase (right) of the hologram. (b) Phase distributions of the reconstructing PSFs used for obtaining the three best-in-focus reconstructed planes. (c) Corresponding three best-in-focus reconstructed planes along the optical axis. (d) Same as (c) but after the resampling along the horizontal axis. (e) Zoomed-in images of the corresponding best-in-focus reconstructed objects.



(b)



(c)



(d)

Fig. 8. (Color online) Fluorescence 3-D imaging by MVP holography [36]: (a) Optical system for acquiring 3×3 perspective projections simultaneously using the macrolens array shown in Fig. 3. Part of the objects in the scene are fluorescently labeled. (b) Composite image plane of the macrolens array acquired by the camera. (c) Magnitude (left) and phase (right) of the nonfluorescence 2-D DIMFH. Two additional fluorescence 2-D DIMFHs are generated as well. (d) Three best-in-focus multicolor reconstructed planes. Viewing this figure in color online is highly recommended.

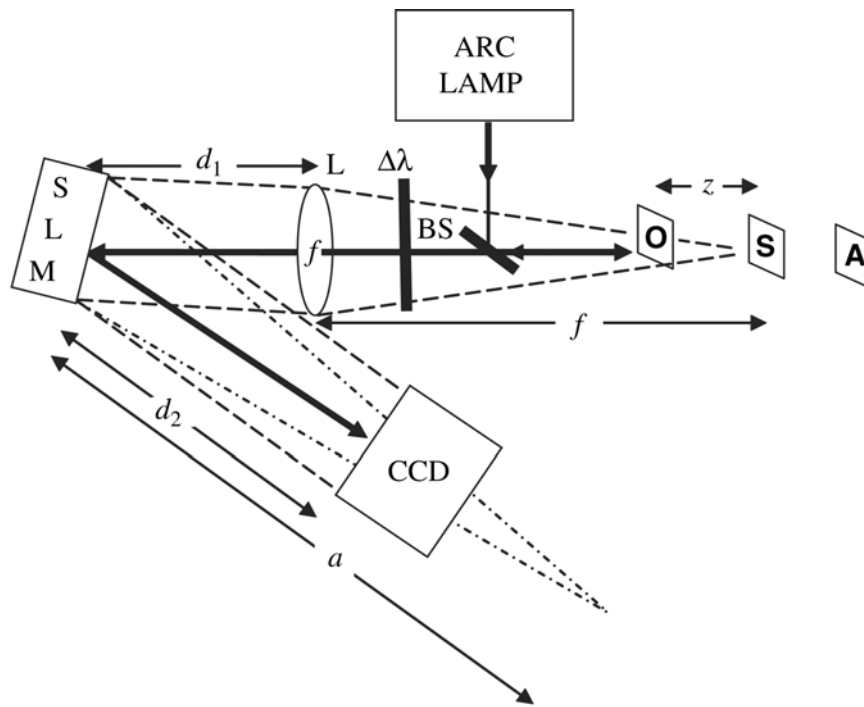


Fig. 13. Schematic of FINCH recorder. BS: beam splitters; SLM: spatial light modulator; CCD: charge-coupled device; L is a spherical lens with $f = 25$ cm focal length. $\Delta\lambda$ indicates a chromatic filter with a bandwidth of $\Delta\lambda = 60$ nm.

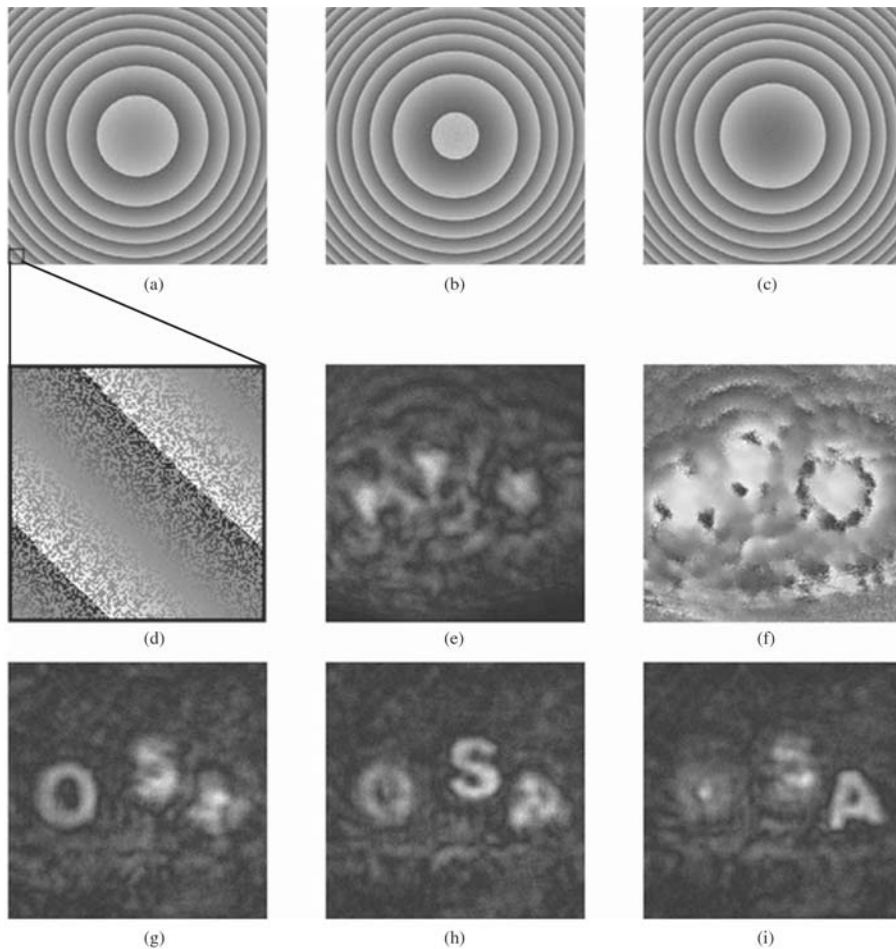


Fig. 14. FINCH results: (a) Phase distribution of the reflection masks displayed on the SLM, with $\theta = 0^\circ$, (b) $\theta = 120^\circ$, (c) $\theta = 240^\circ$. (d) Enlarged portion of (a) indicating that half (randomly chosen) of the SLM's pixels modulate light with a constant phase. (e) Magnitude and (f) phase of the on-axis digital hologram. (g) Reconstruction of the hologram of the three letters at the best focus distance of 'O.' (h) Same reconstruction at the best focus distance of 'S,' and (i) of 'A.'

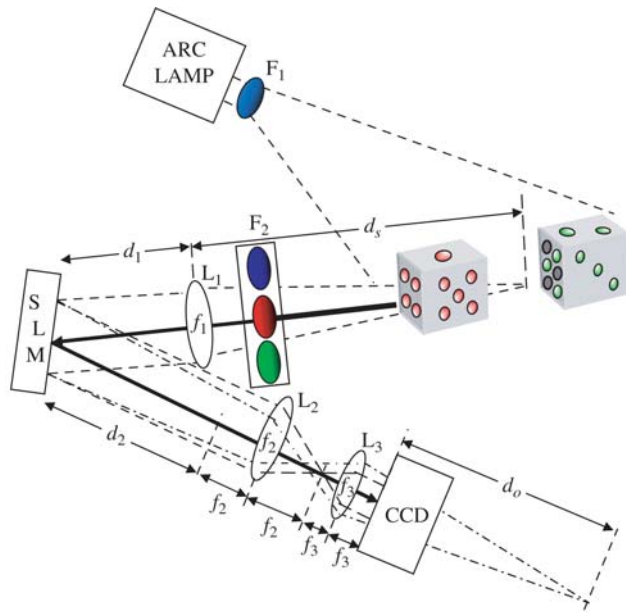


Fig. 15. Schematics of the FINCH color recorder. SLM: spatial light modulator; CCD: charge-coupled device; L_1 , L_2 , L_3 are spherical lenses and F_1 , F_2 are chromatic filters.

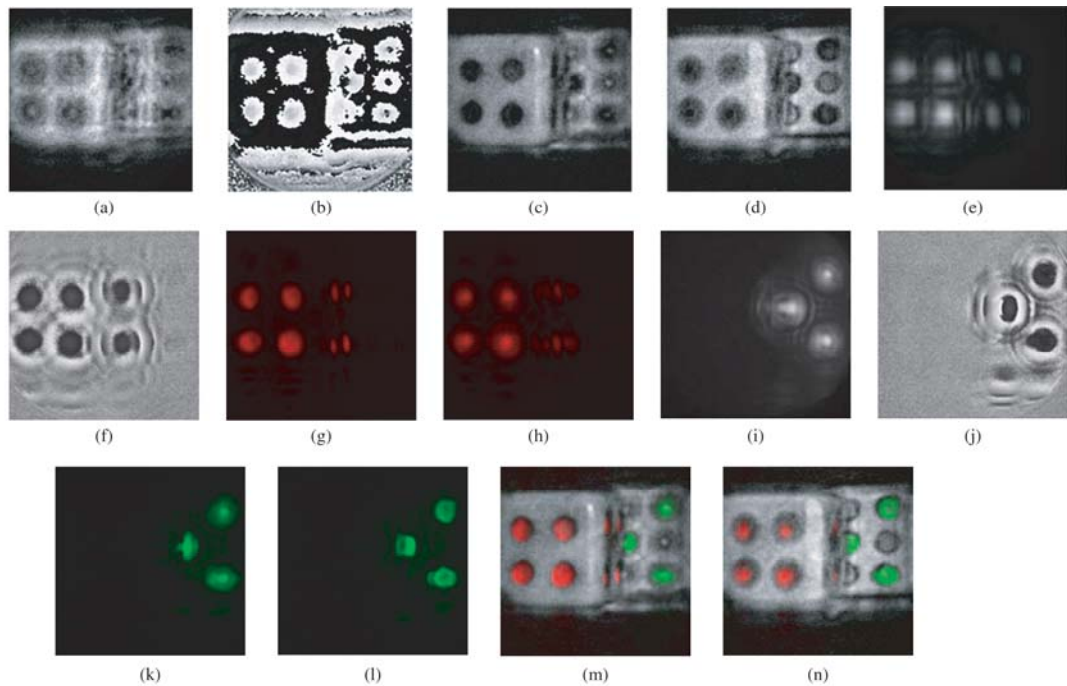


Fig. 16. (a) Magnitude and (b) phase of the complex Fresnel hologram of the dice. Digital reconstruction of the non-fluorescence hologram: (c) at the face of the red-dots on the die, and (d) at the face of the green dots on the die. (e) Magnitude and (f) phase of the complex Fresnel hologram of the red dots. Digital reconstruction of the red fluorescence hologram: (g) at the face of the red-dots on the die, and (h) at the face of the green dots on the die. (i) Magnitude and (j) phase of the complex Fresnel hologram of the green dots. Digital reconstruction of the green fluorescence hologram: (k) at the face of the red-dots on the die, and (l) at the face of the green dots on the die. Compositions of Figures 16(c), (g), and (k) and Figures 16(d), (h), and (l) are depicted in Figures 16(m) and (n), respectively.